

CAUSTIC AND WEAK LENSING ESTIMATORS OF GALAXY CLUSTER MASSES

ANTONALDO DIAFERIO,¹ MARGARET J. GELLER² AND KENNETH J. RINES³

Draft version November 11, 2018

ABSTRACT

There are only two methods for estimating the mass distribution in the outer regions of galaxy clusters, where virial equilibrium does not hold: weak gravitational lensing and identification of caustics in redshift space. For the first time, we apply both methods to three clusters: A2390, MS1358 and Cl 0024. The two measures are in remarkably good agreement out to $\sim 2h^{-1}$ Mpc from the cluster centers. This result demonstrates that the caustic technique is a valuable complement to weak lensing. With a few tens of redshifts per $(h^{-1}\text{Mpc})^2$ within the cluster, the caustic method is applicable for any $z \lesssim 0.5$.

Subject headings: cosmology: miscellaneous – cosmology: observations – galaxies: clusters: individual (Abell 2390, Cl 0024+1654, EMSS 1358+6254) – gravitational lensing

1. INTRODUCTION

The relative distributions of mass and light in the universe have remained a profound and central mystery in cosmology for more than seventy years. Since Zwicky’s pioneering use of the virial theorem to discover dark matter in the Coma cluster (Zwicky 1933), the range and sophistication of methods for estimating cluster masses and mass profiles have increased to include a host of dynamical measures, X-ray estimates and strong and weak gravitational lensing determinations.

Different mass estimators applied to rich clusters of galaxies constrain the mass distribution on different scales. Strong lensing generally provides constraints on very small scales ($\lesssim 0.1h^{-1}$ Mpc). Virial mass estimates, including Jeans’ analysis, assume dynamical equilibrium and apply only within the virial radius. Mass estimates based on X-ray observations assume hydrostatic equilibrium and rarely extend beyond one-half of the virial radius (Majerowicz, Neumann, & Reiprich 2002; Pratt & Arnaud 2002).

At larger clustrocentric radii where equilibrium assumptions break down, there exist only two techniques for mass estimation: weak lensing (Kaiser, Squires, & Broadhurst 1995) and the redshift-space caustic technique (Diaferio & Geller 1997; Diaferio 1999, D99 hereafter). Both techniques enable determination of the mass distribution from the cluster center to distances larger than the virial radius.

The caustic technique has been applied to many local clusters (Rines et al. 2003 and references therein). At small clustrocentric radii, caustic estimates agree well with the traditional virial analyses in the optical and X-ray bands. At larger radii, the caustic technique is still valid, but its mass estimates were tested against N -body simulations only (D99).

Here we discuss the first comparison of mass estimates

¹ Dipartimento di Fisica Generale “Amedeo Avogadro”, Università degli Studi di Torino, Via P. Giuria 1, I-10125, Torino, Italy, diaferio@ph.unito.it

² Smithsonian Astrophysical Observatory, 60 Garden St., Cambridge, MA 02138, USA, mjpg@cfa.harvard.edu

³ Yale Center for Astronomy and Astrophysics, Yale University, P.O. Box 208121, New Haven, CT 06520-8121, USA, krines@astro.yale.edu

from the caustic technique and weak lensing. Only recently have sufficient lensing and spectroscopic data become available to make this comparison. Both techniques have known systematic uncertainties: these comparisons test the importance of these systematics.

In this Letter, we examine mass profile measurements for three intermediate redshift clusters: A2390, MS1358+6254, and Cl 0024+1654.

2. THE CAUSTIC TECHNIQUE

Cluster galaxies plotted in a redshift space diagram (line-of-sight velocity v vs. projected distances R from the cluster center) distribute in a characteristic trumpet shape. The boundaries of this trumpet are called caustics (Kaiser 1987; Regös & Geller 1989). By assuming spherical symmetry and hierarchical clustering for the formation of the large-scale structure, the caustic mass estimator relates the caustic amplitude, the trumpet width in v at each radius R , $\mathcal{A}(R)$, to the escape velocity from the gravitational potential well generated by the cluster.

The procedure developed by D99 provides an automatic method for locating the caustics and determining their amplitude. First, the procedure arranges all the galaxies in the field in a binary tree and finds the cluster members. The cluster members determine the center of the cluster, its one-dimensional velocity dispersion $\langle v^2 \rangle^{1/2}$, and its radius $\langle R \rangle$, the mean projected distance of the members from the cluster center. Table 1 lists these quantities for the three clusters.

The procedure next determines the threshold κ which enters the caustic equation $f_q(R, v) = \kappa$. Here, $f_q(R, v)$ is the galaxy density distribution in the redshift diagram, smoothed with an adaptive kernel. The parameter q sets the scaling between the quantities R and v . We choose the parameter κ by minimizing the quantity $S(\kappa, \langle R \rangle) = |\langle v_{\text{esc}}^2 \rangle_{\kappa, \langle R \rangle} - 4\langle v^2 \rangle|^2$, where $\langle v_{\text{esc}}^2 \rangle_{\kappa, \langle R \rangle} = \int_0^{\langle R \rangle} \mathcal{A}^2(R) \varphi(R) dR / \int_0^{\langle R \rangle} \varphi(R) dR$ is the mean caustic amplitude within $\langle R \rangle$ and $\varphi(R) = \int f_q(R, v) dv$.

D99 shows that the three-dimensional cumulative mass profile can now be estimated as

$$GM(< r) = \frac{1}{2} \int_0^r \mathcal{A}^2(R) dR. \quad (1)$$

The error bars on individual data points are propor-

TABLE 1
 CLUSTER PARAMETERS

cluster	FOV ($\alpha \times \delta$)	$N_{\text{field}} \in [z_1, z_2]$	N	α	δ	z	$\langle v^2 \rangle^{1/2}$	R	r_s	c	r_{200}
A2390	43'8 × 7'4	351 ∈ [0.1, 0.4]	210	21 ^h 53 ^m 35 ^s .53	17°42' 3''16	0.2284	1154	0.85	0.14 ± 0.17	11 ± 12	1.5 ± 2.4
MS1358	20'9 × 21'4	360 ∈ [0.1, 0.5]	282	13 ^h 59 ^m 49 ^s .65	62°30'55''87	0.3289	996	0.76	0.14 ± 0.09	7.7 ± 4.3	1.1 ± 0.9
Cl 0024	20'0 × 24'3	399 ∈ [0.3, 0.5]	251	0 ^h 26 ^m 35 ^s .90	17° 9'41''10	0.3941	937	0.74	0.12 ± 0.11	8.6 ± 7.7	1.0 ± 1.3

NOTE. — Col. 2: Field of view (FOV); Col. 3: no. of galaxies in the FOV within the redshift range $[z_1, z_2]$; Col. 4: no. of members; Cols. 5-7: cluster center coordinates; Col. 8: cluster velocity dispersion; Col. 9: cluster size; Cols. 10-12: NFW fit parameters. Celestial coordinates are J2000. Velocities are in km s^{-1} , lengths in h^{-1} Mpc.

tional to the inverse of the galaxy number density within the caustics (D99). This recipe quantifies the uncertainty in the mass estimate which mostly results from deviations from spherical symmetry. The recipe was calibrated on N -body simulations (Kauffmann et al. 1999) that generally showed less cleanly defined caustics than in the real Universe. Therefore, we suspect that these uncertainties are smaller for real clusters than in the simulations. The small scatter ($\lesssim 30\%$) around the equivalence relation between X-ray and caustic masses (Rines et al. 2003) suggests that the simulations indeed overestimate the errors in the caustic technique at small radii. If 30% represents a rough estimate of the correct caustic mass uncertainty at all radii, the D99 recipe typically overestimates this uncertainty by a factor of two. Nevertheless, because it is the only available prescription for evaluating the error, we use the conservative D99 prescription. Comparison of gravitational lensing and caustic measurements for large samples of clusters in the redshift range 0.2-0.8 will test the accuracy of this recipe.

3. MASS COMPARISON

Mass profile estimates of high-redshift clusters depend on the assumed cosmological parameters: physical distances, X-ray and weak lensing cumulative mass profiles scale as the angular diameter distance D_A . Moreover, if one derives a best-fitting Navarro, Frenk, & White (1997) (NFW) density profile $\rho(r, z) = \delta_c \rho_{\text{crit}}(z) (r/r_s)^{-1} (1 + r/r_s)^{-2}$, with $\rho_{\text{crit}}(z) = 3H^2(z)/8\pi G$ the critical density of the Universe, $H^2(z) = H_0^2[\Omega_0(1+z)^3 + (1-\Omega_0-\Omega_\Lambda)(1+z)^2 + \Omega_\Lambda]$, $\delta_c = c^3(200/3)[\ln(1+c) - c/(1+c)]^{-1}$ and $c = r_{200}/r_s$ the concentration parameter, c also depends (non-linearly) on D_A , because $\delta_c \rho_{\text{crit}}(z)$ scales as D_A^{-2} . Below, all quantities assume $\Omega_0 = 0.3$, $\Omega_\Lambda = 0.7$ and $H_0 = 100h \text{ km s}^{-1} \text{ Mpc}^{-1}$.

Figure 1 shows the redshift diagrams of the three clusters with the caustic location (upper panels) and the mass profiles estimated with the caustic technique, gravitational lensing and X-ray data (middle and lower panels). Gravitational lensing measures all the mass projected onto the sky along the line of sight. Therefore, we distinguish between three-dimensional (middle panels) and projected (lower panels) cumulative mass profiles. Radial distances are three-dimensional (r) or projected onto the sky (R).

The solid lines in Figure 1 show the best-fitting NFW profile with parameters listed in Table 1. To compute these fits, we only used the data points within $r_{\text{lim}} = 1h^{-1}$ Mpc, a conservative radius beyond which the NFW mass profile might not be a good description

of the actual profile. For all clusters, the data points beyond $1h^{-1}$ Mpc do indeed agree with the NFW model, indicating that the correct choice of r_{lim} is irrelevant. In any case, the fit parameters and their errors are only indicative, because the individual data points are correlated. Moreover, the NFW fit parameters are correlated even with independent data points. Keeping one of the two parameters, c or r_s , fixed in our fits reduces their relative errors to $\sim 10\%$.

For each cluster, we also show the best fits determined from the weak lensing (dashed lines) and X-ray (dotted lines) measurements. We now comment on each cluster separately.

A2390 is a rich cluster at $z = 0.228$ with optical (Le Borgne et al. 1991; Yee et al. 1996) X-ray (Böhringer et al. 1998; Allen, Ettori, & Fabian 2001) and both weak (Squires et al. 1996) and strong (Pelló et al. 1991; Pierre et al. 1996) gravitational lensing observations.

Squires et al. (1996) compare the weak lensing data within $\sim 260''$ with a singular isothermal model with velocity dispersion $\sigma = 1093 \text{ km s}^{-1}$ taken from Carlberg et al. (1996). The isothermal model underpredicts the amount of mass actually measured in the range $0.46 - 0.67h^{-1}$ Mpc (left-bottom panel in Figure 1); however, this model is in good agreement with the best-fitting NFW mass profile derived by Allen et al. (2001) from *Chandra* observations. They find $r_s = 0.44_{-0.22}^{+0.76}h^{-1}$ Mpc, $c = 3.6_{-1.6}^{+2.0}$ and $r_{200} = 1.6_{-1.1}^{+2.9}h^{-1}$ Mpc.

By using the galaxy redshift survey by Yee et al. (1996) and by assuming dynamical equilibrium, Carlberg et al. (1996) estimate a mass $M(< 3.3h^{-1}\text{Mpc}) = (2.7 \pm 0.4) \times 10^{15}h^{-1}M_\odot$. The caustic mass $(1.4 \pm 1.2) \times 10^{15}h^{-1}M_\odot$ and the mass $1.8 \times 10^{15}h^{-1}M_\odot$ extrapolated from the weak lensing isothermal model are 48% and 33% smaller than this virial mass, but within its 3σ uncertainty.

At smaller radii, A2390 sports spectacular arcs and arclets (Pelló et al. 1991), some of which have measured redshifts (Bézecourt & Soucail 1997; Frye & Broadhurst 1998; Pelló et al. 1999). Pierre et al. (1996) use the brightest strongly lensed arc and its surrounding shear to derive the projected total enclosed mass $M(< 97h^{-1}\text{kpc}) = (8.0 \pm 1.0) \times 10^{13}h^{-1}M_\odot$ ⁴ (solid diamond in Figure 1), in agreement with the mass $(1.2 \pm 0.7) \times 10^{14}h^{-1}M_\odot$ implied by the projection of the NFW fit

⁴ In this Letter, we rescale each strong lensing mass found in the literature by the effective lensing distance $D_l D_{ls}/D_s$ appropriate to a universe with $\Omega_0 = 0.3$ and $\Omega_\Lambda = 0.7$; D_l , D_s and D_{ls} are the angular distances to the cluster, to the source of the lensed image and between the cluster and the source, respectively.

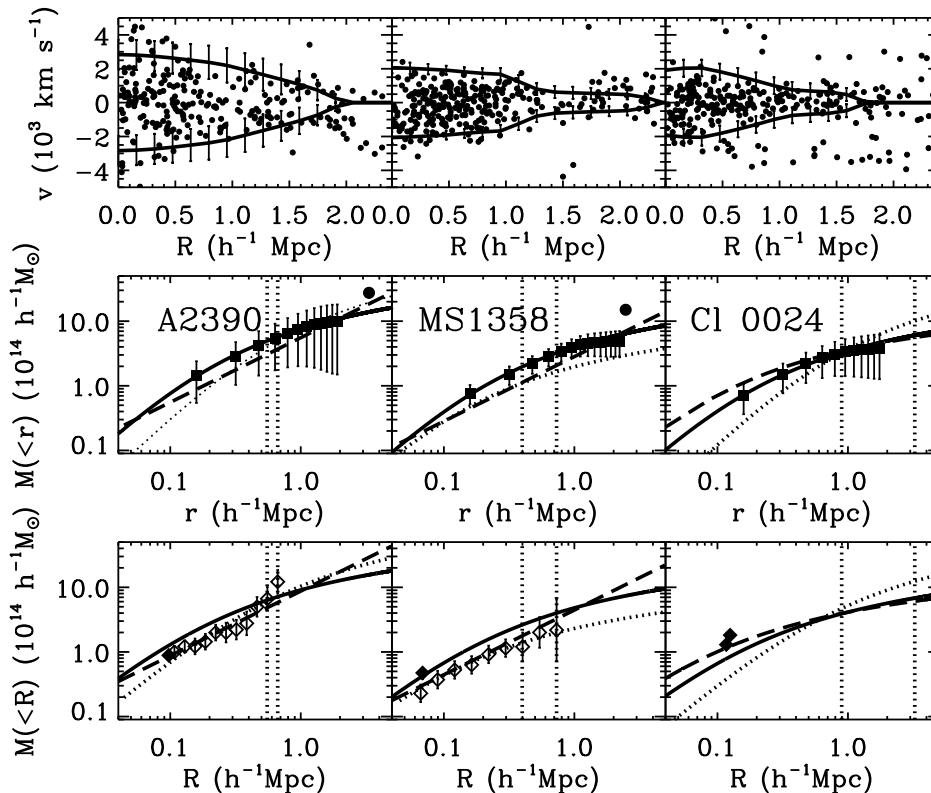


FIG. 1.— The left, middle and right columns are for A2390, MS1358 and Cl 0024, respectively. *Top panels:* Redshift diagrams with the galaxies (dots) and caustic locations (solid lines). Line-of-sight velocities v are in the cluster rest-frame. *Middle panels:* Three-dimensional cumulative mass profiles. The solid squares show the caustic mass estimates; the solid lines are the best-fitting NFW profiles to the data points within $1h^{-1}$ Mpc; the dotted lines are the best-fitting NFW profiles to the X-ray measures (from left to right: Allen et al. 2001; Arabadjis et al. 2002; Ota et al. 2004); the dashed lines are the best-fitting isothermal (A2390, Squires et al. 1996; MS1358, Hoekstra et al. 1998) or NFW models (Cl 0024, Kneib et al. 2003) to the gravitational lensing measures. The left and right vertical dotted lines show the radius of the X-ray and gravitational lensing fields of view, respectively. The two filled circles show the virial estimates by Carlberg et al. (1996) of A2390 and MS1358. *Bottom panels:* Projected cumulative mass profiles; lines are as in the middle panels. The open diamonds show the weak lensing measures: A2390, Squires et al. (1996); MS1358, lower limit by Hoekstra et al. (1998) to the mass profile. Filled diamonds show the strong lensing measures: A2390, Pierre et al. (1996); MS1358: Allen (1998) from the measurement by Franx et al. (1997); Cl 0024: upper symbol, Tyson et al. (1998), lower symbol, Broadhurst et al. (2000). Error bars in all panels are $1-\sigma$; error bars on points where they seem to be missing are smaller than the symbol size.

to the caustic mass; the strong lensing mass also agrees with the mass $8.5 \times 10^{13} h^{-1} M_{\odot}$ implied by the weak lensing isothermal model, and is just above the 68% confidence bound derived with the X-ray analysis (Figure 8 of Allen et al. 2001).

Pierre et al. (1996) derive the strong lensing mass by assuming that the arc is a single lensed galaxy at $z = 0.913$. Frye & Broadhurst (1998) later showed that the fainter part of this arc actually is a second lensed galaxy at $z = 1.033$. The redshifts of the arcs and arclets, which are available now but not at the time of Pierre et al.'s analysis, urges a reformulation of the lensing model of the core of A2390. However, we expect that a newly derived mass will not substantially differ from the mass of Pierre et al. (1996), because the mass estimated with the simplest lensing models, which provide the most inaccurate measures, probably are within 30% of the true value (Kochanek, Schneider & Wambsganss 2003).

MS1358+6254 is a very rich cluster first discovered by Zwicky & Hartog (1968). We collect 381 redshifts in the cluster region from the surveys of Fabricant, McClintock, & Bautz (1991), Fisher et al. (1998) and Yee et al. (1998).

Hoekstra et al. (1998) used HST observations to construct a weak lensing map of the cluster extending to a radius of $\sim 220'' = 0.73h^{-1}$ Mpc. They only derive a lower limit to the mass profile and find a best-fitting singular isothermal model with $\sigma = 780 \pm 50$ km s $^{-1}$ (dashed lines in Figure 1). More recently, Arabadjis, Bautz, & Garmire (2002) analyze a *Chandra* observation of the cluster. They approximate the mass profile within $\sim 2' = 0.4h^{-1}$ Mpc with an NFW profile, with $r_s = 88^{+92}_{-47} h^{-1}$ kpc, $c = 9.3^{+3.8}_{-2.5}$ and $r_{200} = 0.81^{+0.92}_{-0.49} h^{-1}$ Mpc.

Carlberg et al. (1996) assume virial equilibrium to estimate $M(< 2.5h^{-1}\text{Mpc}) = (1.5 \pm 0.2) \times 10^{15} h^{-1} M_{\odot}$ from their galaxy redshift survey. This mass is more than $3-\sigma$ above the weak lensing isothermal extrapolation $7.0 \times 10^{14} h^{-1} M_{\odot}$ which agrees with the caustic estimate $(6.5 \pm 2.8) \times 10^{14} h^{-1} M_{\odot}$. The extrapolation of the X-ray fit yields $3.0 \times 10^{14} h^{-1} M_{\odot}$, a factor of two smaller than the caustic mass and a factor of five below the virial mass. Probably, the assumption of virial equilibrium at this large distance is unrealistic and the extrapolation of the X-ray profile, limited to radii $< 0.4h^{-1}$ Mpc, is unreliable.

In the very central region, Allen (1998) uses the strong lensing observations by Franx et al. (1997) to derive a projected mass $M(< 69h^{-1}\text{kpc}) = 4.4 \times 10^{13}h^{-1}M_{\odot}$ with a 20% uncertainty. The projected NFW profile derived from the caustics yields a perfectly consistent mass $(4.2 \pm 1.3) \times 10^{13}h^{-1}M_{\odot}$. The projected profiles derived by Hoekstra et al. (1998) and Arabadjis et al. (2002) imply the somewhat lower masses $3.0 \times 10^{13}h^{-1}M_{\odot}$ and $2.9 \times 10^{13}h^{-1}M_{\odot}$, respectively.

The X-ray and weak lensing mass models agree within $\sim 0.8h^{-1}$ Mpc, but underestimate the strong lensing mass derived by Allen (1998). The fact that the weak lensing mass provides only a lower limit to the mass profile and the caustic mass is in excellent agreement with the strong lensing measurement suggests that the caustic mass provides the correct mass profile of MS1358 out to $\sim 2h^{-1}$ Mpc.

Significant tension exists between lensing (Bonnet, Mellier, & Fort 1994; Tyson, Kochanski, & dell'Antonio 1998) and X-ray (Soucail et al. 2000; Ota et al. 2004) mass estimates of the *Cl 0024* cluster. Kneib et al. (2003) combine their weak lensing measurements from wide field imaging with the strong lensing measurement by Broadhurst et al. (2000) to derive the best-fitting NFW profile with $r_s = 54 \pm 2h^{-1}$ kpc, $c = 18.7_{-4.3}^{+7.7}$ and $r_{200} = 1.01_{-0.23}^{+0.41}h^{-1}$ Mpc. According to their Figure 12, the uncertainty in their mass estimate is always $\lesssim 10\%$. Our Figure 1 also shows the NFW profile which fits recent *Chandra* data (Ota et al. 2004). These authors derive the NFW profile from a β -model fit. According to its parameters, we find $r_s = 0.56 \pm 0.02h^{-1}$ Mpc, $c = 1.8 \pm 0.3$ and $r_{200} = 1.02 \pm 0.18h^{-1}$ Mpc. Our caustic estimate lies between the lensing and the X-ray fits at $r < 0.2h^{-1}$ Mpc, but it is in excellent agreement with the lensing estimate outside $\sim 0.5h^{-1}$ Mpc.

In the cluster central region, there are two strong lensing measurements which yield comparable masses. However, the very small errors claimed make them inconsistent with each other: $M(< 0.114h^{-1}\text{Mpc}) = (1.30 \pm 0.04) \times 10^{14}h^{-1}M_{\odot}$ (Broadhurst et al. 2000), and $M(< 0.119h^{-1}\text{Mpc}) = (1.563 \pm 0.002) \times 10^{14}h^{-1}M_{\odot}$ (Tyson et al. 1998). We scaled the mass reported by Tyson et al. (1998) by assuming $z = 1.675$ for the arc, as measured by Broadhurst et al. (2000). By construction, the NFW profile of Kneib et al. (2003) agrees with the former (it yields $M(< 0.114h^{-1}\text{Mpc}) = 1.13 \times 10^{14}h^{-1}M_{\odot}$) and therefore disagrees with the latter (it yields $M(< 0.119h^{-1}\text{Mpc}) = 1.17 \times 10^{14}h^{-1}M_{\odot}$). The caustic profile gives smaller, but consistent, masses in

both cases: $(7.9 \pm 3.8) \times 10^{13}h^{-1}M_{\odot}$ and $(8.5 \pm 4.0) \times 10^{13}h^{-1}M_{\odot}$, respectively. The NFW fit to the X-ray data yields even smaller masses: $3.8 \times 10^{13}h^{-1}M_{\odot}$ and $4.2 \times 10^{13}h^{-1}M_{\odot}$ with a $\sim 30\%$ typical error. Czoske et al. (2002) suggest that the peculiar redshift distribution of the galaxies within $\sim 3.5h^{-1}$ Mpc of the cluster center can be explained by a high-speed collision along the line of sight between Cl 0024 and a less massive cluster. This model implies that the X-ray mass estimate based on dynamical equilibrium is unreliable. Because the caustic and lensing mass estimators are both independent of the dynamical state of the cluster, it is reasonable that they agree with each other but disagree with the X-ray mass.

4. CONCLUSION

For the first time, we compare the only two cluster mass estimators that do not rely on the dynamical equilibrium of the system: weak gravitational lensing and caustics in redshift space. We estimate the caustic mass of A2390, MS1358 and Cl 0024 within $\sim 2h^{-1}$ Mpc of the cluster center. The caustic mass profiles are in very good agreement with the lensing profiles. We confirm that the discrepancy between lensing and X-ray mass in Cl 0024 is probably a consequence of the unrelaxed state of the cluster which invalidates the X-ray analysis.

Weak lensing requires accurate photometric wide-field surveys in excellent seeing; moreover, the cluster sample is somewhat limited to clusters at distances where the lensing signal is sufficiently strong. Weak lensing measures all of the mass projected along the line of sight, resulting in a minimum 20% uncertainty in the cluster mass estimates (de Putter & White 2005). The caustic technique, which requires dense wide-field redshift surveys, provides a complementary measurement of the three-dimensional mass profile of individual clusters at moderate redshift; it also yields robust mass profiles for clusters in the local universe.

Future comparison of these techniques for large samples of clusters, covering a range of redshifts, will constrain systematic uncertainties in the methods and may provide insight into the change in the relative amounts of mass in the infall regions and cluster cores as a function of lookback time.

We thank the referee for noticing a few inaccuracies in the first version of this Letter. We have made use of NASA's Astrophysics Data System and the NASA/IPAC Extragalactic Database (NED) operated by the Jet Propulsion Laboratory, California Institute of Technology, under contract with NASA.

REFERENCES

- Allen, S. W. 1998, MNRAS, 296, 392
 Allen, S. W., Etti, S., & Fabian, A. C. 2001, MNRAS, 324, 877
 Arabadjis, J. S., Bautz, M. W., & Garmire, G. P. 2002, ApJ, 572, 66
 Bézecourt, J., & Soucail, G. 1997, A&A, 317, 661
 Bonnet, H., Mellier, Y., & Fort, B. 1994, ApJ, 427, L83
 Böhringer, H., Tanaka, Y., Mushotzky, R. F., Ikebe, Y., & Hattori, M. 1998, A&A, 334, 789
 Broadhurst, T., Huang, X., Frye, B., & Ellis, R. 2000, ApJ, 534, L15
 Carlberg, R. G., Yee, H. K. C., Ellingson, E., Abraham, R., Gravel, P., Morris, S., & Pritchett, C. J. 1996, ApJ, 462, 32
 Czoske, O., Moore, B., Kneib, J.-P., & Soucail, G. 2002, A&A, 386, 31
 de Putter, R., & White, M. 2005, preprint (astro-ph/0412497)
 Diaferio, A. 1999, MNRAS, 309, 610 (D99)
 Diaferio, A., & Geller, M. J. 1997, ApJ, 481, 633
 Fisher, D., Fabricant, D., Franx, M., & van Dokkum, P. 1998, ApJ, 498, 195
 Fabricant, D. G., McClintock, J. E., & Bautz, M. W. 1991, ApJ, 381, 33
 Franx, M., Illingworth, G. D., Kelson, D. D., van Dokkum, P. G., & Tran, K.-V. 1997, ApJ, 486, L75
 Frye, B., & Broadhurst, T. 1998, ApJ, 499, L115

- Hoekstra, H., Franx, M., Kuijken, K., & Squires, G. 1998, *ApJ*, 504, 636
- Kaiser, N. 1987, *MNRAS*, 227, 1
- Kaiser, N., Squires, G., & Broadhurst, T. 1995, *ApJ*, 449, 460
- Kauffmann, G., Colberg, J. M., Diaferio, A., & White, S. D. M. 1999, *MNRAS*, 303, 188
- Kneib, J.-P., Hudelot, P., Ellis, R. S., Treu, T., Smith, G. P., Marshall, P., Czoske, O., Smail, I., & Natarajan, P. 2003, *ApJ*, 598, 804
- Kochanek, C. S., Schneider, P., & Wambsganss, J. 2003, *Gravitational Lensing: Strong, Weak and Micro*, Proceedings of the 33rd Saas-Fee Advanced Course, edited by G. Meylan, P. Jetzer, and P. North (Springer-Verlag: Berlin), in press
- Le Borgne, J.-F., Mathez, G., Mellier, Y., Pelló, R., Sanahuja, B. & Soucail, G. 1991, *A&AS*, 88, 133
- Majerowicz, S., Neumann, D. M., & Reiprich, T. H. 2002, *A&A*, 394, 77
- Navarro, J. F., Frenk, C. S., & White, S. D. M. 1997, *ApJ*, 490, 493 (NFW)
- Ota, N., Pointecouteau, E., Hattori, M., & Mitsuda, K. 2004, *ApJ*, 601, 120
- Pelló, R., Sanahuja, B., Le Borgne, J.-F., Soucail, G., & Mellier, Y. 1991, *ApJ*, 366, 405
- Pelló et al. 1999, *A&A*, 346, 359
- Pierre, M., Le Borgne, J. F., Soucail, G., & Kneib, J. P. 1996, *A&A*, 311, 413
- Pratt, G. W., & Arnaud, M. 2002, *A&A*, 394, 375
- Rines, K., Geller, M. J., Kurtz, M. J., & Diaferio, A. 2003, *AJ*, 126, 2152
- Regös, E., & Geller, M. J. 1989, *AJ*, 98, 755
- Soucail, G., Ota, N., Böhringer, H., Czoske, O., Hattori, M., & Mellier, Y. 2000, *A&A*, 355, 433
- Squires, G., Kaiser, N., Fahlman, G., Babul, A., & Woods, D. 1996, *ApJ*, 469, 73
- Tyson, J. A., Kochanski, G. P., & dell'Antonio, I. P. 1998, *ApJ*, 498, L107
- Yee, H. K. C., Ellingson, E., Abraham, R. G., Gravel, P., Carlberg, R. G., Smecker-Hane, T. A., Schade, D., & Rigler, M. 1996, *ApJS*, 102, 289
- Yee, H. K. C., Ellingson, E., Morris, S. L., Abraham, R. G., & Carlberg, R. G. 1998, *ApJS*, 116, 211
- Zwicky, F. 1933, *Helvetica Phys. Acta*, 6, 110
- Zwicky, F., & Herzog, E. 1968, *Catalogue of Galaxies and Clusters of Galaxies*, Vol. VI (Pasadena: Caltech)